




Dissolution Behaviors of Various Carbonaceous Materials in Liquid Iron: Interaction Between Graphite and Iron

MIN-MIN SUN,¹ JIAN-LIANG ZHANG,^{1,2} KE-JIANG LI ^{1,4},
SHAN REN,^{3,5} ZI-MING WANG,¹ CHUN-HE JIANG,¹ and
HONG-TAO LI¹

1.—School of Metallurgical and Ecological Engineering, University of Science and Technology Beijing, Beijing 100083, People's Republic of China. 2.—School of Chemical Engineering, The University of Queensland, St Lucia, QLD 4072, Australia. 3.—College of Material Science and Engineering, Chongqing University, Chongqing 400044, People's Republic of China. 4.—e-mail: likejiang@ustb.edu.cn. 5.—e-mail: shan.ren@cqu.edu.cn

The dissolution behaviors of carbon into iron and the interface characteristics were observed by a high-speed CCD camera and a scanning electronic microscope with energy disperse spectroscopy. Samples were obtained from two flexible and simple experiments: (1) the static drop method and (2) the iron cover method. The results show that carbon dissolution occurs when iron is still in solid form, leading to the decrease of the melting point from 1780 K (pure iron) to 1497 K (carburized iron). Carbon dissolved from graphite forms small irregular flake-like structures, then transforms into large-size dendritic crystals by intergrowth with the C added to the iron before heating. Compared with C atoms moving into iron, it is more difficult for Fe atoms to move up into graphite due to the strong repulsive force of the Fe-Fe bond. It is found that the thickness of the Fe-C interface is about 200 μm , which does not change with the initial C content of the iron-carbon alloy.

INTRODUCTION

Resource limitation and environmental deterioration have led to a greater focus on the tracking of material flow and energy flow, especially of carbon, which is closely related to energy consumption and global warming. Since 2000, global steel production and demand has dramatically increased, and carbonaceous materials as the carriers for both energy and emissions burn fiercely.¹ Iron-carbon interactions have long been the subject of interest to ironmakers and steelmakers. Fe-C interactions appear in different ferrous metallurgical processes, such as the carburization of coke and chars in hot metal in blast furnaces (BF),² and carbon brick eroded by molten iron.³ An in-depth understanding of the dissolution behaviors of various carbonaceous materials in liquid iron is significant for the optimization of ironmaking.^{4,5} The utilization of resources and the reduction of environmental pollution can also be improved.

Carbon in BF hot metal is mainly from the dissolution of coke and chars, with a very little from carbon bricks. Understanding the interaction between coke and molten iron is essentially important for reducing the coke rate by increasing the utilization of other alternative fuels.^{6,7} Moreover, the wetting behavior between liquid iron and coke influences the permeability in the BF lower part, which strongly affects the stable operation.^{8,9} The dissolution of carbon-based refractories in the hearth is inevitable. To prolong the life of the furnace and ensure the safety of the production operation, slower dissolution rates of carbon-based refractories into molten iron are preferred.^{10–12}

Currently, the investigation on the carbon dissolution into hot metal can be divided into three aspects. First are the effects of carbon structure and crystallinity on the carbon dissolution rate. The results show that it is easier for highly-ordered C materials to dissolve in iron compared to less-ordered ones. And there are no obvious effect of

anisotropic C content on carburization reaction rates, which may be due to the complex nature of bonding across cross-links between the crystallites.^{13–15} Second is the effect of the mineral matter layer formed in the interface between the carbonaceous materials and iron. Minerals in coke have been found to inhibit the dissolution process by gathering at the carbon-iron interface. Some additives, i.e., CaO, MgO, SiO₂ and Al₂O₃, significantly reduce the dissolution of carbon. However, the presence of iron oxide in special coxes is favorable for carburization.^{16–20} And third is the influence of C and S in the melt on carbon dissolution. Studies have shown that a higher initial C concentration results in a smaller width of the interfacial region. While the presence of S slows down the pickup of C, it is also known to deposit in the form of CaS at the iron side, creating interfacial blockages. As the C and S atoms tend to displace each other to regions of low concentrations, it has been assumed that this position exchange takes place through the Fe atoms.^{19,21–25}

In general, the existing research mainly lies in the factors affecting the dissolution reaction and carburization rate. Understanding about the interface phenomena during the carbon dissolution process is still scarce, such as the Fe and C atoms migration behavior within the interface, the wettability of iron on carbon materials, etc. In addition, little research exists on the effect of the initial C on the interface phenomenon of the molten iron and carbon materials. Therefore, a project dedicated to the analysis of the dissolution behavior of carbon materials (coke and carbon bricks) into iron was established. As a first report, the simplest form of carbon, graphite, was chosen to lay a solid foundation for studying the carburization of coal/coke/char in the iron and steel production process. Two simple and ingenious methods were used to study the interaction between the carbon material and the molten iron. The influence of the initial carbon content C_0 in the iron on the interface behavior was also examined. Research on non-graphite materials will be carried out in the next stage. The results show that C dissolved into iron leads to the decrease of the melting point. Carbon from graphite forms small irregular flake-like graphite structures, and they transform into large-size dendritic crystals when bonding to the initial carbon. The Fe-C interfacial layer thickness does not change with C_0 of iron-carbon alloy.

MATERIALS AND METHODS

In order to investigate the effect of carbon dissolution behavior on the interface between graphite and iron, two kinds of experiments were conducted. One was the static drop method, while the other was the iron cover method. The first method utilizes a high-speed CCD camera to visualize the carbon dissolution process in real time. Thus, the starting

melting temperature of iron, the contact angle between iron and graphite, and the dissolution depth between liquid iron and graphite can be obtained by analyzing the real-time images. Since iron powder and carbon powder can be used in the second method, it is very easy to adjust the initial carbon content in the liquid iron. Therefore, the focus of the second method is to investigate the influence of the initial carbon on the carbon dissolution process and to provide supplementary information to characterize the reaction process.

Experimental Sample

In this study, solid industrial pure iron in lumps and reduced iron powder were used to obtain liquid iron, while commercial graphite was chosen as the carbon resources for both the carburizer and the Fe-C alloy. Detailed information about the raw materials is shown in Table S1 (see supplementary material).

Experimental Procedure

The schematic illustration for both measurements is shown in Fig. 1, and the detailed experimental procedures are introduced below. The heating modes of the two experimental methods are shown in Figure S1 (see supplementary material). The cross-sections of the solidified specimens were cut and polished and observed in order to investigate the microstructural morphologies and crystalline structure by scanning electron microscopy with energy dispersive spectroscopy (SEM-EDS).

1. Static drop method

A horizontal tube furnace was used for the static drop method; the furnace has a sapphire window to allow in situ measurements of the dissolution process and wetting behavior (see supplementary Figure S2). The substrate was made of graphite powder with particle sizes less than 200 μm , under a pressure of 8 MPa in a cuboid die. The volume density and porosity of graphite substrate are 1.83 g/cm³ and 16%, respectively. At the start, the graphite substrate and industrial iron block were

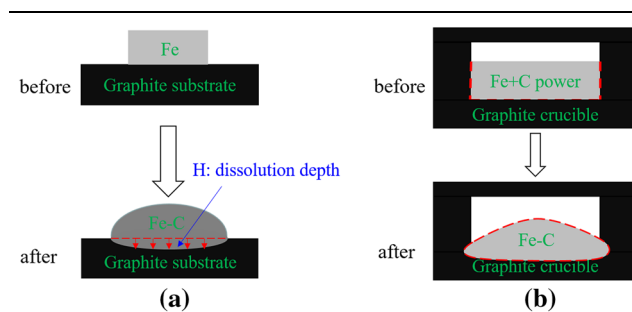


Fig. 1. Schematic illustration showing the dissolution process of different experimental methods: (a) static drop method and (b) iron cover method.

put into the horizontal tube furnace, as shown in Fig. 1a. Before heating, the furnace was ventilated with 2 L/min high-purity argon for 10 min. The dynamic images of metal droplet impacts on the solid surfaces were captured by the high-speed CCD camera.

2. Iron cover method

A covered graphite crucible ϕ 18 mm made by the same molding method was selected for the iron cover method. Reduced iron powder with 0, 1, 2, 3, 4, and 5 wt% graphite powder was added to the crucible as shown in Fig. 1b, then the crucible was put into the muffle furnace. It was ventilated for 20 min (27 L in the muffle furnace) with 5 L/min high-purity argon before heating. The identification methods of the original interfaces between the graphite and iron can be seen in Figure S3 (see supplementary material).

RESULTS AND DISCUSSION

Influence of Dissolution on the Melting Behavior of Iron

To investigate the influence of carburization on the melting behavior of iron, a corundum substrate was used for the static drop method. The melting process of iron with the corundum and graphite substrates at different temperatures are shown in Fig. 2a, b, respectively. It is obvious that the presence of C had a significant impact on the melting of the iron. The obtained image was then identified by the small difference of the serial photograph using the analysis software, Image J, and the melting point of iron on the corundum and graphite substrates is the temperature at which the sample height is reduced by 3%. The melting temperature of the industrial pure iron on corundum substrate was as high as 1780 K, while it reduced to 1497 K for the graphite substrate. With the dissolution of the C, the melting point of iron is

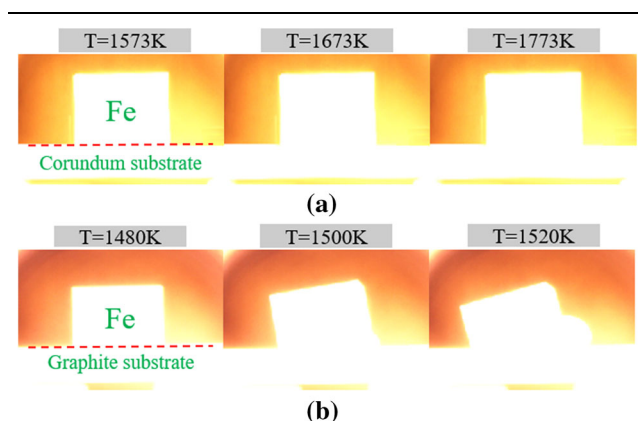


Fig. 2. Captured image sequences of the melting behavior of iron under different substrate materials: (a) corundum and (b) graphite.

reduced by 283 K. According to Ohno et al.,²⁶ the carburization starts at a lower temperature when the iron is still in a solid state. When the carbon content of iron at the Fe-C interface reaches 4.40% at 1479 K, the liquid phase begins to be produced according to the Fe-C binary diagram. As the temperature increases, the rate of carbon diffusion increases making the iron melt and expand.

Figure 3 shows the macroscopic and microscopic morphology of the samples after carbon dissolution by the static drop method. There are some small iron droplets on the surface due to the existence of certain pores in the graphite substrate, as shown in Fig. 3a; this phenomenon was also observed by Nguyen et al.⁸ The cross-section shows a regular morphology after the dissolution of the graphite into the iron, which corresponds to the simulation results by Yin et al.²⁷ First, the solid iron starts with a contraction in the horizontal direction and a protrusion in the vertical direction; then, the contraction continues, creating the iron with a half-moon shape; after that, the iron continuously spreads out in the horizontal direction until an equilibrium is reached; the spreading ability is a representation of the wettability. This proved the hypothesis that the wettability of the iron droplets is dominantly influenced by the top atoms at the very beginning. By microscopic image analysis of Fig. 3b, the dissolution depth reached about $700 \pm 10 \mu\text{m}$ and the wetting angle was about $109.6^\circ \pm 1^\circ$, which is close to the calculated results (107.9° – 112.6°) by Yin et al.,²⁷ and the measured results (107° – 111°) by Fiona et al.²⁸

Evolution of Iron-Carbon Interface

The microscopic morphology of the sample following the iron cover method is shown in Fig. 4a. The inner wall of the graphite crucible was seriously corroded by molten iron, and the precipitation of the C in the iron depended on the distance from the interface. Carbon near the interface layer formed small irregular flake-like graphite structures similar to the C in the cast iron, and its content gradually decreased away from the interface. Well-formed large-size dendritic graphite has also been found. The solubility and final morphology of the C into the iron may depend on the Si saturation of the

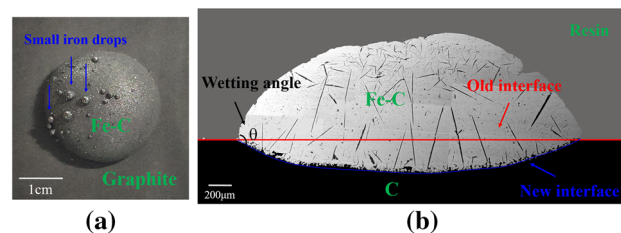


Fig. 3. Optical and SEM morphology images of samples after carbon dissolution by the static drop method: (a) a macro-view from the top of Fe-C; (b) backscattered SEM picture of the dissolution interface between graphite and iron.

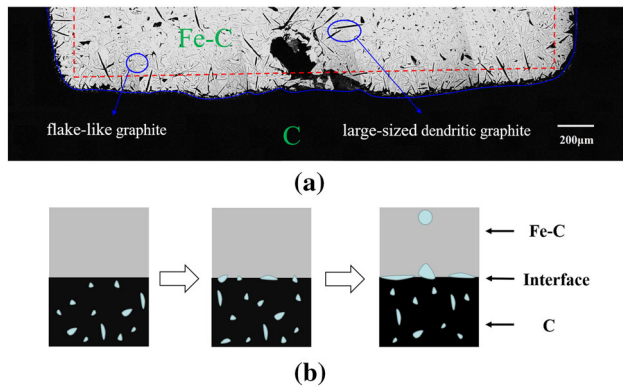
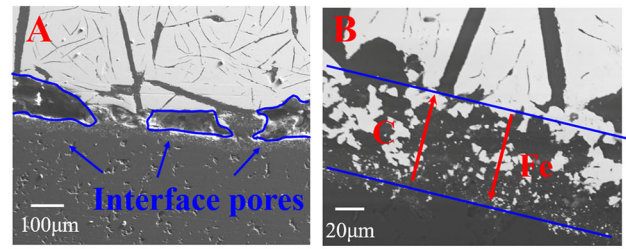


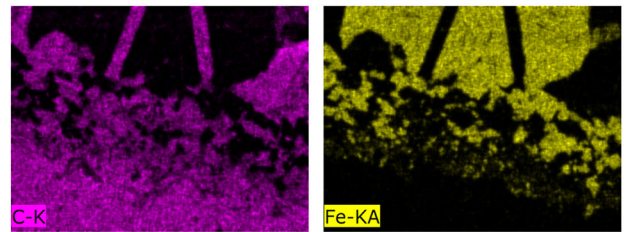
Fig. 4. Results of the iron cover method: (a) backscattered SEM image of the dissolution of graphite into molten iron (C_0 in iron is 2 wt%); (b) schematic diagram of the formation of the spacer at the Fe-C interface.

molten iron, and carbon is easier to dissolve into iron under-saturated with Si, which corresponds to the results of Li et al.²⁹ and Gornostayev et al.³⁰ This suggests that the well-ordered carbon can be produced by the dissolution reaction of C by molten iron and the precipitation reaction. With the increase of carbon content by the dissolution reaction, the small graphite crystals transformed into large-sized dendritic crystals in a later recrystallization step by the intergrowth and aggregation with the graphite powder added earlier to make the Fe-C alloy.³¹ In combination with the physical characteristics and the carburizing process of the graphite crucible, the formation process of the spacer at the Fe-C interface is shown in Fig. 4b. The gradual dissolution of the carbon led the pores in the graphite to be exposed at the Fe-C interface, which ultimately separated the iron and graphite. Bubbles rose when the effect of buoyancy was greater than that of other forces, eventually forming droplets in the surface of the iron.

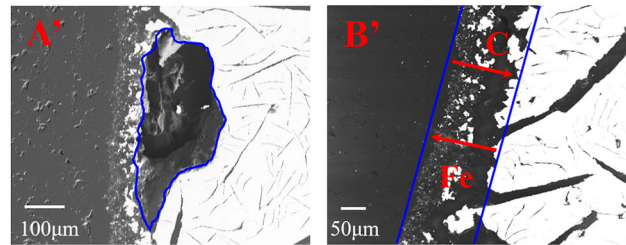
As shown in Fig. 5, the SEM micrographs demonstrate that the presence of pores at the interface formed the apparent spacer. Figure 5a indicates that there were C atoms moving into the iron, and that it was more difficult for the Fe atoms to move up into the graphite. There are a small number of volatiles in the graphite since, in hot-pressed bricks, the volatiles disappear and the pores are formed at a high temperature. The pore diameter increases due to some of the carbon being oxidized at high temperature. Therefore, pores were observed between the Fe and C. In addition, it is also observed that the mutual penetration depth of the Fe and C atoms acted differently between the bottom and the side wall, which may be caused by the gravity of the molten iron. Due to the rapid diffusion of carbon at high temperatures, the distribution of carbon remains the same for the bottom and side of the graphite crucible. The Fe-C interface layer thickness is discussed in detail below.



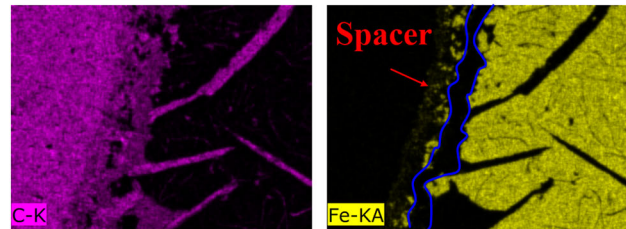
EDS maps of B:



(a)



EDS maps of B':



(b)

Fig. 5. SEM micrographs and EDS maps showing the interaction between iron and graphite: (a) bottom and (b) side of graphite crucible.

Effects of Initial Carbon in Iron on Interaction

It is observed in Fig. 4a that the original Fe-C interface shape changed from rectangular to circular by the dissolution reaction. And the radius of the circular was different with C_0 in iron, which can be used as an indicator for the degree of carburization, as shown in Fig. 6. The result shows that the dissolution chamfer radius decreased with the increase of C_0 in iron from $1533 \pm 74 \mu\text{m}$ (0 wt% C_0) to $860 \pm 48 \mu\text{m}$ (5 wt% C_0). The greater the C_0 , the less the C iron needed to reach saturation, leading to a smaller dissolution depth. However, the dissolution chamfer reached $487.5 \mu\text{m}$ even when the C_0 is 5 wt% (hot metal with 5 wt% C is supersaturated at 1773 K), which indicated that

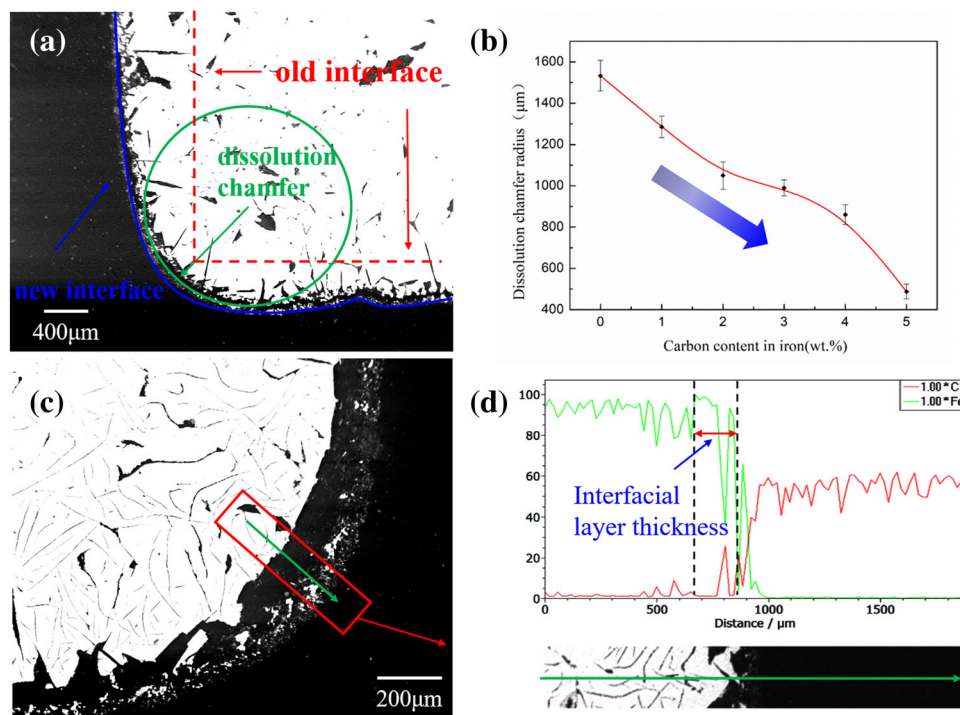


Fig. 6. Influence of C_0 in iron on the degree of dissolving and the characterization of interfacial thickness by EDS line scanning: (a) characterization of dissolution degree by the dissolution chamber; (b) dissolution degree changed with C_0 in iron; (c) backscattered map of the interface between iron and graphite, and (d) line scan method to calculate the interface layer thickness (C_0 in iron is 2 wt%).

the dissolution process is a dynamic equilibrium at high temperature with atomic diffusion for both Fe and C.

In order to study the influence of C_0 on the interfacial behavior, the interfacial layer thickness of Fe-C dissolution was measured approximately using the line scan analysis method of EDS. The content distribution changes of Fe and C in the vertical direction of the interface were quantified to characterize the interfacial thickness, as shown in Fig. 6c. The average interfacial layer thickness was obtained by multiple measurements at different locations.

Once a C atom is dissociated from the graphite, it diffused easily into the melt. The Fe atoms, however, were found to be difficult to move into the graphite. Due to the order of repulsive force being Fe-Fe bond > Fe-C bond > C-C bond, the movement of C atoms into the melt lowered the energy of the whole system. Therefore, the Fe atom movement to replace the C atoms of an attractive C-C bond was not easy. Figure 7 shows the variation of the interfacial layer thickness with the C_0 in iron. As can be seen, the thickness of the Fe-C dissolution interface did not change with C_0 , even when the C_0 in iron was 5 wt%. This indicates that, although the C_0 in iron was related to the dissolved amount of C in the iron, which formed different dissolution depths, the mutual diffusion of Fe and C atoms did not depend on C_0 at all. At 1773 K, the thickness

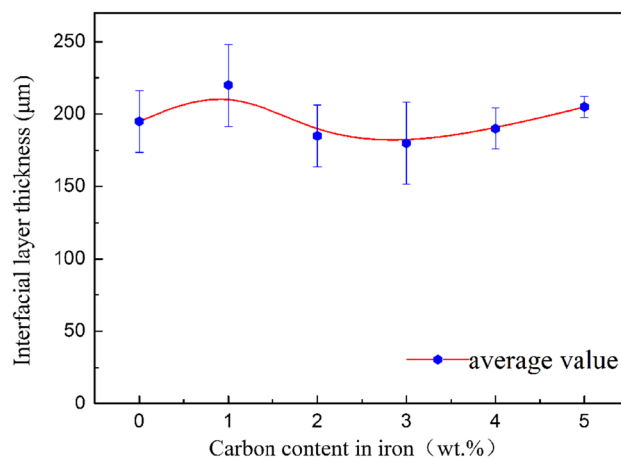


Fig. 7. The variation of the interface layer thickness with the initial carbon content, C_0 , in iron.

of the interfacial layer of carbon and iron diffusion is about 200 μm for different C_0 . Sahajwalla et al.²¹ found a slight reduction in the width of the interfacial region with increasing C content of the melt by Monte Carlo algorithms, but the tiny difference exists between 2 atomic layers when the carbon content in iron changes from 0 wt% to 2 wt%. This phenomenon may become an important characteristic of carbon dissolution in iron, which needs to be further verified on the dissolution behavior of different carbon materials.

CONCLUSION

The dissolution behavior of graphite carbon into iron was studied by means of the static drop method and iron cover experiments, combined with SEM-EDS analysis. The experimental results are as follows:

1. The dissolution of carbon into iron can occur at a low temperature when the iron is still in solid state, which leads to the melting point of iron decreasing from 1780 K to 1497 K. The dissolution depth reached about $700 \pm 10 \mu\text{m}$ and the wetting angle was about $109.6^\circ \pm 1^\circ$.
2. After the completion of carburization, C from different sources precipitates in different ways when cooling. Carbon dissolved from graphite forms small irregular flake-like structures. The small graphite crystals will transform into large-size dendritic crystals by the intergrowth and aggregation with the C powder added to the iron before the experiment.
3. The dissolution chamfer radius decreases with the increase of C_0 in the iron from $1533 \pm 74 \mu\text{m}$ (0 wt% C_0) to $860 \pm 48 \mu\text{m}$ (5 wt% C_0). Due to the larger repulsive force of the Fe-Fe bond, it is more difficult for Fe atoms to move up into the graphite than C atoms to migrate into molten iron which eventually forms the Fe-C interfacial layer. The thickness of the interfacial layer between the graphite and the Fe-C alloy is about $200 \mu\text{m}$ at 1773 K, and does not change with the C_0 in the iron, which may become an important characteristic of carbon dissolution.

ACKNOWLEDGEMENTS

This work was part of a research project named "The dissolution behavior and carburizing ability of coke dissolution in hot metal" supported by the National Science Foundation of China (51774032); the National Science Foundation for Young Scientists of China (51804025); the National Key Research and Development Program of China (2017YFB0304300 and 2017YFB0304303); the Chinese Fundamental Research Funds for the Central Universities (FRF-TP-17-086A1).

ELECTRONIC SUPPLEMENTARY MATERIAL

The online version of this article (<https://doi.org/10.1007/s11837-019-03664-9>) contains supplementary material, which is available to authorized users.

REFERENCES

1. M. Sun, X. Ning, J. Zhang, K. Li, G. Wang, and H. Wang, *Chin. Metall.* 28, 1 (2018).
2. K. Li, R. Khanna, J. Zhang, Z. Liu, V. Sahajwalla, T. Yang, and D. Kong, *Fuel* 133, 194 (2014).
3. K. Jiao, X. Fan, J. Zhang, K. Wang, and Y. Zhao, *Ceram. Int.* 44, 19981 (2018).
4. K. Li, J. Zhang, Z. Liu, X. Ning, and T. Wang, *Ind. Eng. Chem. Res.* 53, 5737 (2014).
5. X. Wang, *Metallurgy of Iron and Steel, Part I: Ironmaking*, 2nd ed. (Beijing: Metallurgical Industry Press, 2013), pp. 42–49.
6. D. Jang, Y. Kim, M. Shin, and J. Lee, *Metall. Mater. Trans. B* 43, 1308 (2012).
7. R. Khanna, F. Mccarthy, H. Sun, N. Simento, and V. Sahajwalla, *Metall. Mater. Trans. B* 36, 719 (2005).
8. C.S. Nguyen, K. Ohno, T. Maeda, and K. Kunitomo, *ISIJ Int.* 57, 1491 (2017).
9. C.S. Nguyen, K. Ohno, T. Maeda, and K. Kunitomo, *ISIJ Int.* 56, 1325 (2016).
10. F. Zhang, *J. Iron. Steel Res. Int.* 20, 53 (2013).
11. S. Zhang, H. Yan, *5th Int. Cong. on Science and Technology of Ironmaking*, Beijing, 13, 201 (2009).
12. Z. Liu, J. Zhang, H. Zuo, and T. Yang, *ISIJ Int.* 52, 1713 (2012).
13. K. Ohno, A. Babich, J. Mitsue, T. Maeda, D. Senk, H.W. Gudenau, and M. Shimizu, *ISIJ Int.* 52, 1482 (2012).
14. C. Wu and V. Sahajwalla, *Metall. Mater. Trans. B* 31, 243 (2000).
15. M.W. Chapman, *Insoluble oxide product formation and its effect on coke dissolution in liquid iron*, the University of Wollongong, Doctoral Dissertation, 72 (2009).
16. S.T. Cham, R. Khanna, V. Sahajwalla, R. Sakurovs, and D. French, *ISIJ Int.* 49, 1860 (2009).
17. B.J. Monaghan, M.W. Chapman, and S.A. Nightingale, *Steel Res. Int.* 81, 829 (2010).
18. R. Khanna, V. Sahajwalla, B. Rodgers, and F. McCarthy, *Metall. Mater. Trans. B* 37, 623 (2006).
19. M.W. Chapman, B.J. Monaghan, S.A. Nightingale, J.G. Mathieson, and R.J. Nightingale, *Metall. Mater. Trans. B* 39, 418 (2008).
20. H. Gudenau, J. Mulanza, and D. Sharma, *Steel Res.* 61, 97 (1990).
21. V. Sahajwalla and R. Khanna, *Metall. Mater. Trans. B* 31, 1517 (2000).
22. V. Sahajwalla and R. Khanna, *Acta Mater.* 50, 663 (2002).
23. F. Mccarthy, R. Khanna, V. Sahajwalla, and N. Simento, *ISIJ Int.* 45, 1261 (2005).
24. F. McCarthy, V. Sahajwalla, J. Hart, and N. Saha-Chaudhury, *Metall. Mater. Trans. B* 34, 573 (2003).
25. Y. Deng, J. Zhang, and K. Jiao, *ISIJ Int.* 58, 815 (2018).
26. K. Ohno, T. Maeda, K. Nishioka, and M. Shimizu, *ISIJ Int.* 50, 53 (2010).
27. Y. Yin, W. Li, H. Shen, J. Zhou, H. Nan, M. Deng, X. Shen, and Z. Tu, *ISIJ Int.* 58, 1022 (2018).
28. F. Mccarthy, *Interfacial phenomena and dissolution of carbon from chars into liquid iron during pulverised coal injection in a blast furnace*. University of New South Wales, Doctoral Dissertation, 88 (2004).
29. K. Li, J. Zhang, Z. Liu, M. Barati, J. Zhong, M. Wei, G. Wang, and K. Jiao, T. Yang. *Metall. Mater. Trans. B* 46, 1104 (2015).
30. S.S. Gornostayev, T.M. Fabritius, O. Kerkkonen, and J.J. Harkki, *Int. J. Miner. Metall. Mater. B* 19, 478 (2012).
31. W. Wang, K.M. Thomas, R.M. Poultney, and R.R. Willmers, *Carbon* 33, 1525 (1995).

Publisher's Note Springer Nature remains neutral with regard to jurisdictional claims in published maps and institutional affiliations.